11

Modeling Wind Speed for Power System Applications

Noha Abdel-Karim, Marija Ilic and Mitch J. Small
Carnegie Mellon University
USA

1. Introduction

The intermittent nature of wind power presents special challenges for utility system operators when performing system economic dispatch, unit commitment, and deciding on system energy reserve capacity. Also, participation of wind power in future electricity markets requires more systematic modeling of wind power. It is expected that the installed energy capacities from wind sources in the United States will increase by up to 20% by the year 2020. New York Independent System Operator (NYISO), General Electric (GE), and Automatic Weather Stations Inc., (AWS) conducted a project for the future of wind energy integration in the United States. They stated that NY State has 101 potential wind energy sites and it should be able to integrate wind generation up to at least 10% of system peak load without further expansion (GE report 2005). In order to integrate wind power systematically, it is necessary to solve the technical challenges as well as policy regulation designs. Some of these polices have been updated to allow increased intermittent renewable energy by settling imbalances in generation rulemakings and portfolio standards, where the most commonly used one at this time is the production tax credit portfolios.

Due to intermittent nature of wind power, forecasting methods become a powerful tool and of great importance to many power system applications that include uncertainties in generation outputs. The recent work has discussed several methods to develop wind power forecasting algorithms to anticipate the degrees of uncertainty and variability of wind generation. (C. Lindsay & Judith, 2008) use an auto-regressive moving average model to estimate the next ten-minute ahead production level for a hypothetical wind farm and investigate the possibility of pairing wind output with responsive demand to reduce the variability in the net wind output. In (Kittipong M. et al., 2007), the authors develop an Artificial Neural Network (ANN) model to forecast wind generation power with 10-min resolution. Current and previous wind speed and wind power generation are used as input parameters to the network where the output from the ANN is the wind generation power. (M. S. Miranda & R. W. Dunn, 2006) predicted one-hour-ahead of wind speed using both an auto-regressive model and Bayesian approach. (D. Hawkins & M. Rothleder, 2006), discuss operational concerns with increased amount of wind energy in the Day-ahead- and Hour-ahead-Market for CAISO in California. They emphasize the importance of forecasting accuracy for unit commitment and ancillary services and the implications of load following or supplemental energy dispatch to rebalance the system every five minutes. In (Alberto F. at el., 2005), the authors propose a probabilistic method to estimate the forecasting error for

a Spanish Electricity System. They propose cost assessment with wind energy prediction error. The assessment is developed to estimate the cost associated with any energy deviation they cause. (Dale L. Osborn, 2006) discusses the impact of wind on the LMP market for Midwest MISO at different wind penetrations level. His LMP calculations decrease with the increase of wind energy penetration for the Midwest area. The authors of (Cameron W. Potter at el., 2005) describe very short-term wind prediction for power generation, utilizing a case study from Tasmania, Australia. They introduce an Adaptive Neural Fuzzy Inference System (ANFIS) for short-term forecasting of a wind time series in vector form that contains both wind speed and wind direction.

We next describe our modeling approach to derive a family wind models ranging from short through and long term models. Using the same data, we illustrate achievable accuracy of this model. This chapter presents three major parts in sections 2, 3 and 4. First, section 2 presents a short term wind speed linear prediction model in state space representation using linear predictive coding (LPC), FIR and IRR filters. 10-minute, one-hour, 12-hour, and 24-hour wind speed predictions are evaluated in least square error sense and the prediction coefficients are then used in the state space stochastic formula representing past and future predicted values. One year wind speed data in 10 minute resolution are first fitted by two Weibull distribution parameters and then transformation to normal distribution is done for prediction calculation purposes.

Second, section 3 of the chapter models wind speed patterns by decomposing it in different time scales / frequency bands using the Fourier Transform. The decomposition ranges from hourly (high frequency) up to yearly (low frequency), and are important in many power grid applications. Short, medium and long-term wind speed trends require data analysis that deals with changing frequencies of each pattern. By applying Fourier analysis to wind speed signal, we aim to decompose it into three components of different frequencies, 1) Low Frequency range: for economic development such as long term policies adaptation and generation investment (time horizon: many years), 2) Medium Frequency range: for seasonal weather variations and annual generation maintenance (time horizon: weeks but not beyond a year), 3) High frequency range: for Intra-day and Intra-week variations for regular generation dispatches and generation forced outage (time horizon: hours but within a week). Each decomposed signal is presented in a lognormal distribution model and a Discrete Markov process and the aggregated complete wind speed signal is also applied.

Third, section 4 presents the prediction results using past histories of wind data, which support validity of Markov model. These independencies have been modeled as linear state space discrete Markov process. A uniform quantization process is carried to discretize the wind speed data using an optimum quantization step between different state levels for both wind speed distributions used. Also state and transition probability matrices are evaluated from the actual representation of wind speed data. Transition probabilities show smooth transitions between consecutive states manifested by the clustering of transition probabilities around the matrix diagonal.

2. Wind speed prediction model

2.1 Wind data distribution models

This prediction model uses more than 50 thousands samples of one-year wind speed data in 10-minute resolution. The data are used to determine the best fitted parameters of the

Weibull distribution model. Wind speed data are obtained from National weather station in NYISO zonal areas by approximate longitudes and latitudes station's allocation (National weather station, Available online). The empirical cumulative distribution function (CDF) for the wind speed random variable (RV) X has been evaluated using n samples based on the statistical Weibull formula as (Noha Abdel-Karim at el., 2009):

$$\hat{F}_X(x) = \frac{Rank(x)}{n+1} \tag{1}$$

α	Slope β	Standard Error (intercept)	Standard error (slope)	R-square
0.0356	1.77	1.4×10^{-3}	8×10^{-4}	99.4%

Table I. Linear regression defines Weibull distribution parameters

Where a random variable X (R.V) represents wind speed, and "n" is the total sample size. Knowing ahead that the wind speed RV is best characterized by the Weibull distribution model:

$$\begin{aligned} f_X(x) &= \alpha\beta x^{\beta-1} e^{-\alpha x^{\beta}} \\ &= \frac{\beta}{a}\left(\frac{x}{a}\right)^{\beta-1} e^{-\left(x/a\right)^{\beta}} \end{aligned} \tag{2}$$

$$\begin{aligned} F_X(x) &= 1 - e^{-\alpha x^{\beta}} \\ &= 1 - e^{-\left(x/a\right)^{\beta}} \end{aligned} \tag{3}$$

Where in equation (2) or (3), we mention two alternate, yet equivalent forms of Weibull PDF and CDF related by $a = \alpha^{(-1/\beta)}$. Linear regression is performed between $X = \ln(x)$, where x is the data plotted on the horizontal axis, versus the following CDF metric on the vertical axis:

$$Y = \ln\left(-\ln(1-\hat{F}_X(x))\right) \tag{4}$$

It is known that the PDF parameters are related to the linear regression slope m and Y-intercept C, as follows:

$$\begin{aligned} &\beta = slope = m \\ &\alpha = \exp(C) \;\Leftrightarrow a = \exp\left(-C/\beta\right) \end{aligned} \tag{5}$$

The regression results are shown in table I and both empirical and Weibull cumulative distributions are plotted in figure 1.

Figure 1 presents a best Weibull distribution fit with the empirical CDF to wind speed data. The next step is the transformation to normal distribution with mean zero and variance one.

This transformation is used in both the fitting and prediction processes. The histograms of wind speed signals in both Weibull and Normal distributions are shown in Figures 2 and 3, respectively. By looking to Figure 3, the shape of the actual signal is shifted down with the exact pattern due to the normalization process, (Noha Abdel-Karim at el., 2009).

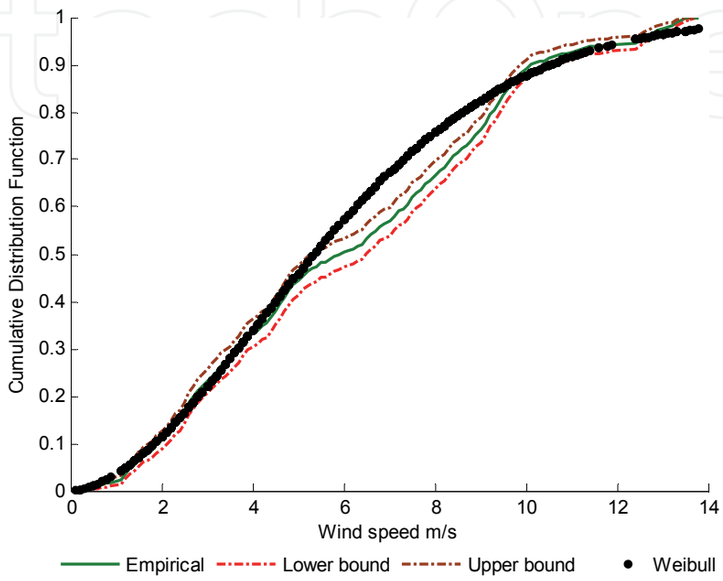

Fig. 1. Empirical and Weibull Cumulative Distribution Functions.

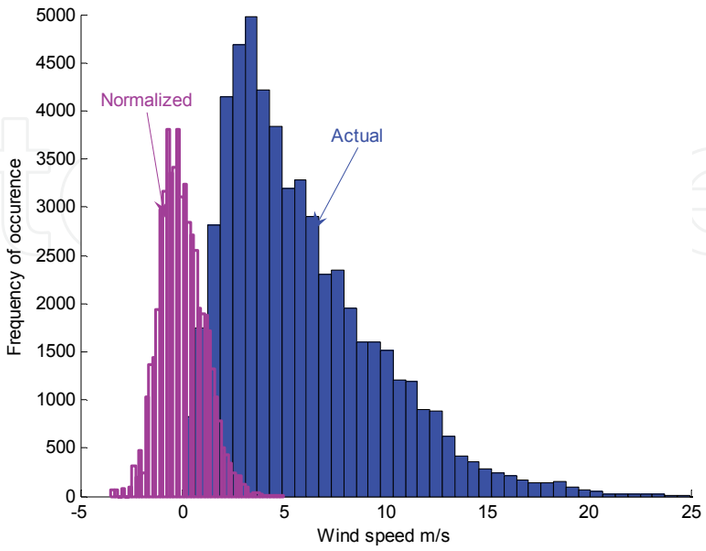

Fig. 2. Actual & normalized frequency occurrence of wind speed data.

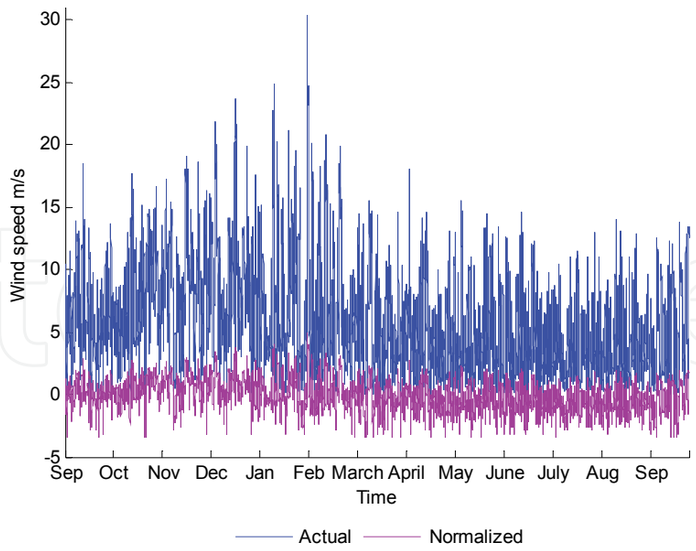

Fig. 3. Actual and normalized wind speed data.

2.2 Normalization of wind speed data

The initial step in the prediction process is data normalization. This step is done by transforming the actual wind speed data X into Normal wind speed data, Xn (i.e., Xn is a normalized Gaussian RV with zero mean and unit variance). This transformation is performed using the Normal CDF inversion as follows:

$$\left.\begin{aligned} F_X(x) &= 1 - e^{-\alpha x^{\beta}} \\ &= F_{X_n}(x_n) = G(0,1) \end{aligned}\right\} \quad \Leftrightarrow \quad x_n = F_{X_n}^{-1}\left(F_X(x)\right) \tag{6}$$

Normal transformation is performed for the sole purpose of prediction, for both the fitting and prediction processes. Figures 2 and 3 show the histograms and time series, respectively, for both the actual (Weibull) wind speed X and Normal wind speed *Xn*. The shape of the Normal signal Xn is shifted down with negative values (Figure 3) compared to the actual signal X due to the normalization process.

2.3 Linear prediction and filter design

This section presents finite impulse response (FIR) and infinite impulse response (IRR) filters. Both filters are being used to determine the prediction coefficients needed to process the normalized wind speed signal x_n, except that we drop the subscript "n" so as not to be confused with the discrete time index. In discrete time, the Z-transform of a signal has been used of a filter as follows:

$$g(n) = \sum_i g_i \delta(n-i) \;\Rightarrow G(z) = \sum_i g_i z^{-i} \qquad \text{(General signal/IIR filter)}$$

$$h(n) = \sum_i^N h_i \delta(n-1) \;\Rightarrow\; H(z) = \sum_{i=0}^N h_i z^{-i} \qquad \text{(FIR filter)}$$

Where δ(n) is the Kronecker delta function. The wind speed random process x(n) is characterized as wide sense stationary (WSS) Gaussian (Normal) process, and hence will remain Gaussian after any stage of linear filtering. However, the wind speed process is NOT white but can be closely modeled as Auto-Regressive (AR) process as will be shown next.

2.4 Linear Predictive Coding (LPC) and Finite Impulse Response Filter (FIR)

For prediction purposes of normalized wind speed data, we use Linear Predictive Coding (LPC) based on the autocorrelation method to determine the coefficients of a forward linear predictor. Prediction coefficients are calculated by minimizing the prediction error in the least squares sense (P. P. Vaidyanathan, 2008). The method provides the LPC predictor and its prediction error as follows:

$$\hat{x}_{LPC}(n) = -\sum_{i=1}^{N} b_i\, x(n-i)$$
$$e_N(n) = x(n) - \hat{x}_{LPC}(n) = x(n) + \sum_{i=1}^{N} b_i\, x(n-i) \tag{7}$$

Where N is defined as the prediction order (using N past data samples) and the coefficients {b1, .., bN} are the fitting coefficients which minimize the mean square (MS) prediction error signal. Yule-Walker (or normal) equations based on autocorrelation matrix have been used to compute those prediction coefficients (P. P. Vaidyanathan, 2008). The LPC predictor has a direct equivalent implementation as an FIR filter if we observe that the error Z-transform is obtained as:

$$\mathrm{E}_N(z) = \mathrm{X}(z) \times \mathrm{B}_N(z) \quad \Rightarrow \quad \mathrm{X}(z) = \mathrm{B}_N^{-1}(z) \times \mathrm{E}_N(z)$$
$$\mathrm{B}_N(z) = 1 + \sum_{i=1}^{N} b_i\, z^{-i} \tag{8}$$

Where BN(z) is the FIR filter transfer function used to compute the output error signal. In other terms, it is also called the prediction polynomial (P. P. Vaidyanathan, 2008). Figure 4 shows how to obtain the output error signal using two equivalent forms: a) LPC prediction and subtraction, and, b) direct FIR filter design, (Noha Abdel-Karim at el., 2009).

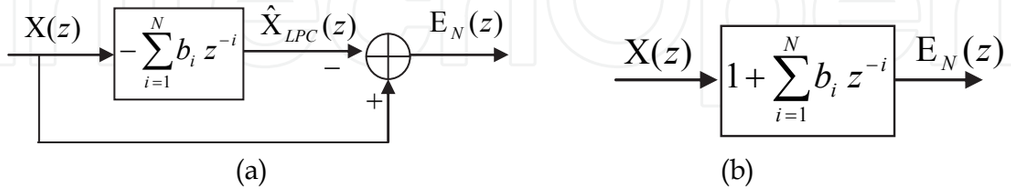

(a) (b)

Fig. 4. Output prediction error signal using: a) LPC prediction and subtraction. b) Direct FIR filter design.

To predict the normalized wind speed data, a forward LPC predictor $\hat{x}_{LPC}(n)$ can certainly be used, but its accuracy is rather poor. However, the main advantage of LPC is that, as the prediction order N increases sufficiently, the prediction error $e_N(n)$ tends to be closely approximated as white noise (P. P. Vaidyanathan, 2008). This helps in modeling the Normal

wind speed as AR signal as will be shown next. Thus, forward LPC is considered an important initial pre-coding step, (Noha Abdel-Karim at el., 2009).

2.5 Auto-Regressive (AR) model prediction and Infinite Impulse Response Filter (IIR) filtering

The true wind speed can be obtained by multiplying the error signal $E_N(z)$ – if it is known – by the inverse of the FIR filter $B_N^{-1}(z)$, (Equation 8), which is now an *all-pole* IIR filter. If the error signal is equivalent to white noise for large prediction order N, then the *z*-multiplication (i.e., convolution or filtering in discrete time) now yields a signal that is modeled as Gaussian Auto-Regressive (AR) process. Figure 5 shows the AR model block diagram, while the reproduced AR signal is obtained by rewriting equation (7) in terms of error as:

$$x(n) = -\sum_{i=1}^{N} b_{i,N}\, x(n-i) + e_N(n) \tag{9}$$

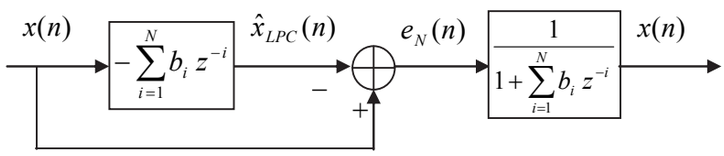

Fig. 5. Auto-regression generation process using LPC estimation method

Equation (9) seems to be an ideal reproduction of $x(n)$ by inversion and it assumes the following:

1. The error signal is exactly updated in real time at the prediction time "n". This is a *genie assisted* condition, as $\hat{x}(n)$ is not available yet!
2. All the true N past data samples are available or exactly estimated (measured) by the wind turbine speed meter and reported on time to the prediction algorithm.
3. The prediction coefficients $\{b_1, \ldots, b_N\}$ are computed using the true past data samples and updated for each new prediction.

In a practical prediction algorithm, these genie conditions do not hold. As for the prediction error, different computation models can be used such as:

1. Prediction error is *estimated* as a random generation of white noise of zero mean & unit variance (P. P. Vaidyanathan, 2008).
2. For initial or limited time intervals, the error can be *exactly computed* using true available data samples to investigate the tracking of the algorithm, but not for long term prediction.
3. The prediction error can be *estimated* from exact measurements but up to a delay of one or more samples, i.e., measurement at time (n – L) applies at time "n". For example, if the prediction update interval is 10 minutes and the measurement delay is 1 hour, then the sample count delay is L = 60/10 = 6 samples. The minimum estimation delay is L = 1.

In our work we excluded the white noise generation alternative and considered the two other alternatives for wind speed forecasting.

2.6 The prediction algorithm for wind speed

2.6.1 Linear prediction phases

More than 50,000 data samples collected in a 10-minute intervals have been used in this short term prediction. A time reference $n = N_S$ has been used which sets the end of known data and start of prediction, where $N_S \leq 50{,}000$ and the remaining samples can be used for tracking the algorithm.

A measurement reporting interval of L samples has been assumed and that there is no error in the measurement or the reporting process. At time epochs $n = N_S + m\,L$, where m is integer, the L measurements $x(n - L + 1)$, $x(n - L + 2)$, …, $x(n)$ are reported and will be available to use at the next epoch, $(N_S + m\,L + 1)$. Depending on L, we have the following extreme cases:

$$L = 1: \rightarrow \text{Point estimator case.}$$

$$L = \infty: \rightarrow \text{Time series case, i.e., no estimation at all.}$$

The following signals and associated time epochs have been defined for prediction purposes as follows:

$x(n)$: True Normal signal known within $0 \leq n \leq N_S$ or whenever measurement is available as above.

$\hat{x}(n)$: Predicted signal using IIR filter or AR recursion.

$x_{REF}(n)$: Reference signal used to produce $\hat{x}(n)$.

$x_{REF}(n) = x(n)$ within $0 \leq n \leq N_S$ or whenever measurement is available

$e_N(n) = x(n) - \hat{x}(n)$: True prediction error, only known if $x(n)$ & $\hat{x}(n)$ are known.

$\hat{e}_N(n)$: Prediction error estimate, either white noise or delayed measurement.

The prediction algorithm can be summarized as follows:

a. ***Training phase*** within $0 \leq n \leq N_S$: Apply the LPC algorithm on the true samples $x(0)$, … , $x(N_S)$ to obtain the prediction coefficients $\{1, b_1, \ldots, b_N\}$. Then we filter the same samples using the FIR coefficients $\{-b_1, \ldots, -b_N\}$ to compute the predictor $\hat{x}(n)$ and true prediction error $e_N(n) = x(n) - \hat{x}(n)$ within $0 \leq n \leq N_S$. Further, we pre-load the reference signal $x_{REF}(n) = x(n)$ within $0 \leq n \leq N_S$.

Prediction phase for $n \geq N_S + 1$: We apply the AR model of equation (9) after computing the error estimate $\hat{e}_N(n)$. We use the same prediction coefficients obtained in the training phase if we plan short-term prediction, which is our case. Otherwise, we have to update the coefficients for long-term prediction. The steps for prediction at epoch "n" are given by:

1. Compute the prediction error estimate using:

$$\begin{aligned} \hat{e}_N(n) &= x_{REF}(n-1) - \hat{x}(n-1) \quad \text{if } x_{REF}(n-1) = x(n-1) \\ &= \hat{x}(n-2) - \hat{x}(n-1) \quad , \text{ if } x_{REF}(n-1) = \hat{x}(n-1) \end{aligned} \tag{10}$$

   We can set $\hat{e}_N(n)$ as randomly generated white noise or also import a snapshot from the past true prediction error series obtained in the training phase.

2. By inspecting equation (9), we compute the predicted signal via the AR recursion:

$$\hat{x}_{AR}(n) = -\sum_{i=1}^{N} b_{i,N}\, x_{REF}(n-i) + \hat{e}_N(n) \tag{11}$$

3. Update the reference signal entries as follows:

$$\text{If n} \neq N_S + m\,L \rightarrow \qquad x_{REF}(n) = \hat{x}_{AR}(n)$$

$$\text{If n} = N_S + m\,L \rightarrow \text{b} \qquad [x_{REF}(n - L + 1),$$

$$x_{REF}(n - L + 2), \ldots, x_{REF}(n)] = [x(n - L + 1), x(n - L + 2), \ldots, x(n)]$$

4. Update the prediction coefficients if needed by running the LPC on the reference signal. It is best to make such update at n = $N_S + m\,L$ because $x_{REF}(n)$ would be just updated by measurements.
5. Increment n and go back to step 1.

Figure 6 shows the two phases of the prediction process

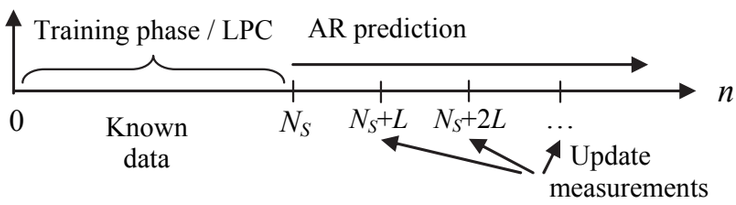

Fig. 6. The two phases of prediction process.

2.6.2 Wind speed prediction results

Wind speed data have been gathered from Dunkirk weather station in the west zone of New York State. Those data have been used for the stochastic prediction of wind speed (National Weather Station, Available online).

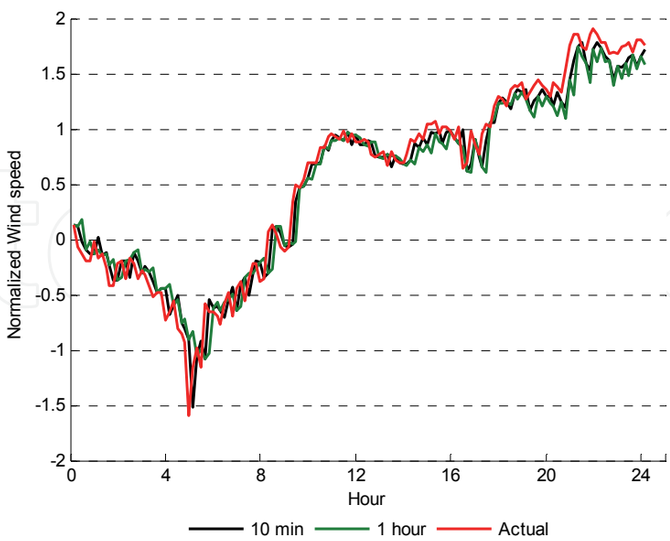

Fig. 7. Ten minutes and one hour prediction using 10 minute past value

Figures 7 and 8 assist remarkable observation that the prediction model insensitive to the prediction order which is defined as the number of observed data (history) used in the

prediction. The 10-minute wind speed prediction model shows persistence for all prediction orders used.

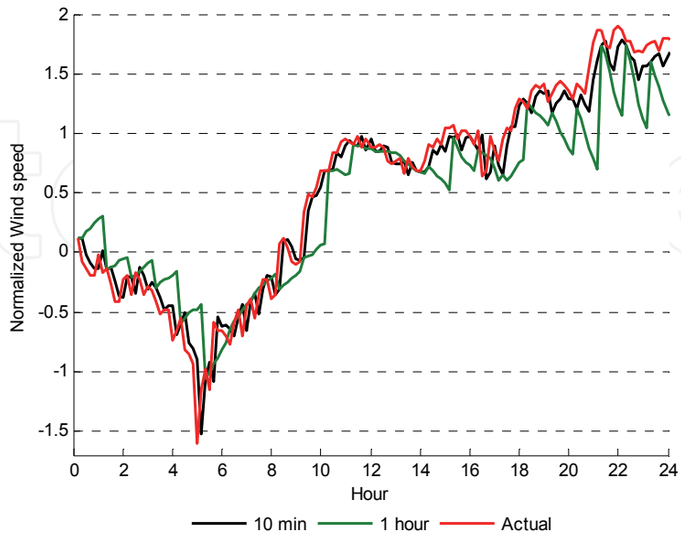

Fig. 8. Ten min and one hour prediction using 1 hour past values

The effect of how the increase in the number of present and past wind speed sample data does not significantly reduce the root mean square error (RMSE), (Figure 9). This led us to an interesting valuation of data structuring and modeling. If only can one recent sample random variable captures stochastic statistics of wind signal to predict future values, then time and memory reductions in presenting such signal can be modeled as a discrete Markov process; the process that stated generally the independencies between past and present values to present signal statistics and structure using state and transition probabilities that will be discussed in detail later.

3. Wind speed signal decomposition

In electricity markets, decisions of utility companies on power selling/buying, production levels, power plants scheduling and investment are made with risks and uncertainties due to volatility and unpredictability of renewable energy patterns. For that, coming up with reasonable modeling of wind speed in different patterns with different time scales, ranging from hours up to few years, are of most importance in many power grid applications. In doing so, different wind signal trends require different data analyses that capture different frequencies. Those frequencies are defined as:

1. Low frequency range: for economic development such as long term policies adaptation and generation investment, (time horizon: many years)
2. Medium frequency range: To detect seasonal weather variations, and therefore help in assigning mid-term generation capacities which influence electricity market prices and power grid generation planning for few weeks with no effect beyond a year.
3. High frequency range: for Intra-day and Intra-week variations for regular generation dispatches and forced generation outage, for fast variations of few hours but not beyond a week.

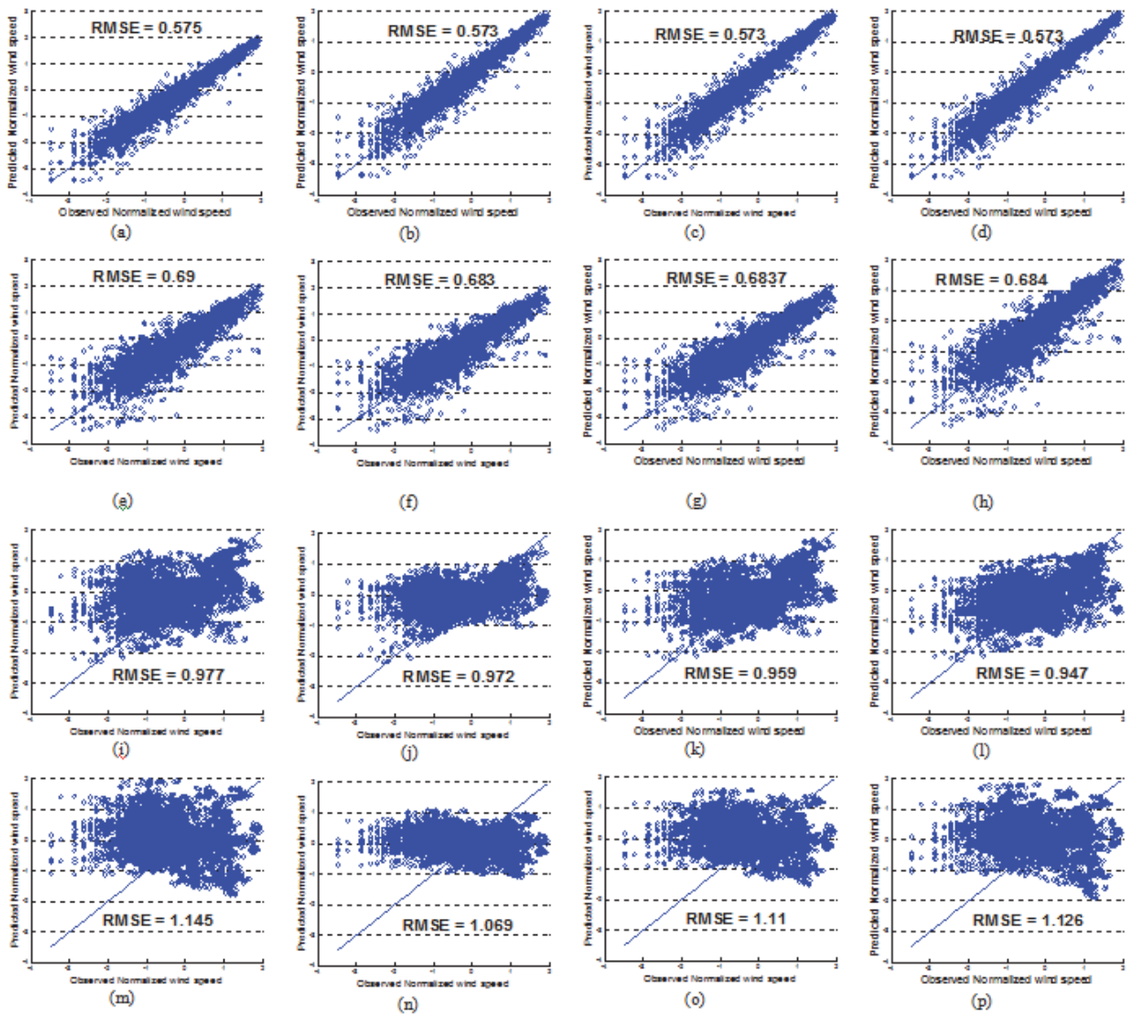

Fig. 9. Wind speed prediction using various past wind speed data in 10 minute resolution:
1st raw: 10 minute prediction using: (a) 10 min, (b) one hour, (c) 12 hours, and (d) 24 hours past data.
2nd raw: 1 hour prediction using: (e) 10 min. , (f) one hour, (g) 12 hours , and (h) 24 hours past data.
3rd raw: 12 hours prediction using: (i) 10 min. , (j) one hour, (k) 12 hours , and (l) 24 hours past data.
4th raw: 24 hours prediction using: (m) 10 min. , (n) one hour, (o) 12 hours , and (p) 24 hours past data.

In this section, short, medium and long-terms wind speed trends have been decomposed by applying Discrete Fourier transform (Yang HE, 2010).
A Discrete Fourier Transform (DFT) X[k], is computed for the natural logarithm of wind speed signal, x[n]. The DFT is then decomposed in frequency domain into low, medium and high frequency components, each of different frequency index range as:

$$X[k] = X_L[k] + X_M[k] + X_H[k] \tag{12}$$

Where $X_L[k]$, $X_M[k]$ and $X_H[k]$ are the low, medium and high frequency components, respectively. The DFT applies only to finite discrete signal (i.e., sequence of length "N").

$$x[n] \quad for \quad 0 \le n \le N-1$$

Where n is a discrete time index. The DFT, X[k], is also a discrete sequence of length "N" and k is a discrete frequency index. The main frequency coefficients for each component are given by:

$$\begin{aligned} X_L[k] &= \begin{cases} X[k] & , 0 \le k \le k_y \\ 0 & , k_y \le k \le N/2 \end{cases} \\ X_M[k] &= \begin{cases} X[k] & , k_y < k \le k_d \\ 0 & , otherwise \end{cases} \\ X_H[k] &= \begin{cases} X[k] & , k_d < k \le N/2 \\ 0 & , 0 \le k \le k_d \end{cases} \end{aligned} \tag{13}$$

It is noted that the DFT X[k] exhibits complex conjugate symmetry around $k = N/2$; hence all the decomposition components in (13) have conjugate symmetric coefficients within $N/2 < k \le N-1$. The thresholds k_y , k_w and k_d are the yearly, weekly and daily discrete frequency indices and are related to their analog frequency values by:

$$\begin{aligned} f_y &= \frac{f_s}{8760} = \frac{k_y f_s}{N} \\ f_w &= \frac{f_s}{168} = \frac{k_w f_s}{N} \\ f_d &= \frac{f_s}{24} = \frac{k_d f_s}{N} \end{aligned} \tag{14}$$

Where f_s = 1 sample/hr is the sampling frequency and N is the sample size covering 16 years from 1994 till 2009 in hourly resolution (National Weather Station, Available online).
Then we take the Inverse DFT (IDFT) of each component in (13), we obtain the aggregated IDFT of (12) in time domain:

$$x_t[n] = x_L[n] + x_M[n] + x_H[n] \tag{15}$$

Each IDFT signal component in (15) is modeled as a Gaussian time series. By taking the exponent of each signal in (15), we obtain the log-normal time domain signals that represent the low, medium and high frequency components of the original wind speed signal. Each pattern can be used to characterize the behavior of wind speed for different purposes. Figure 10 shows the aggregation of the three log-normal wind speed components in the time domain. Each decomposed wind speed signal is of important use in different applications in power systems, e.g., wind power predictions, scheduling and investment decisions.

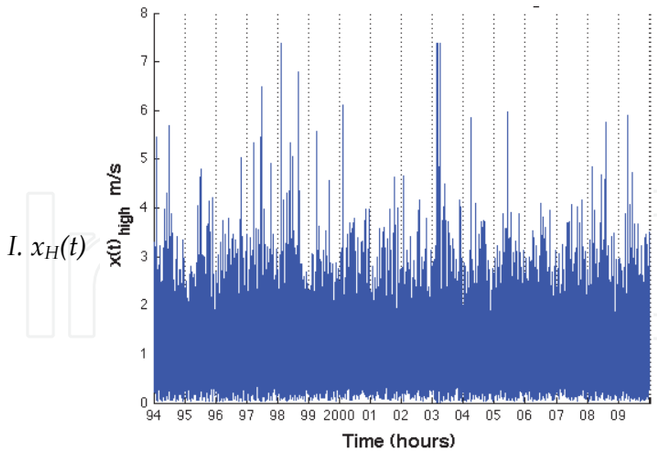

I. $x_H(t)$

$$x_t(t) = x_H(t) + x_M(t) + x_L(t)$$

II. $x_M(t)$

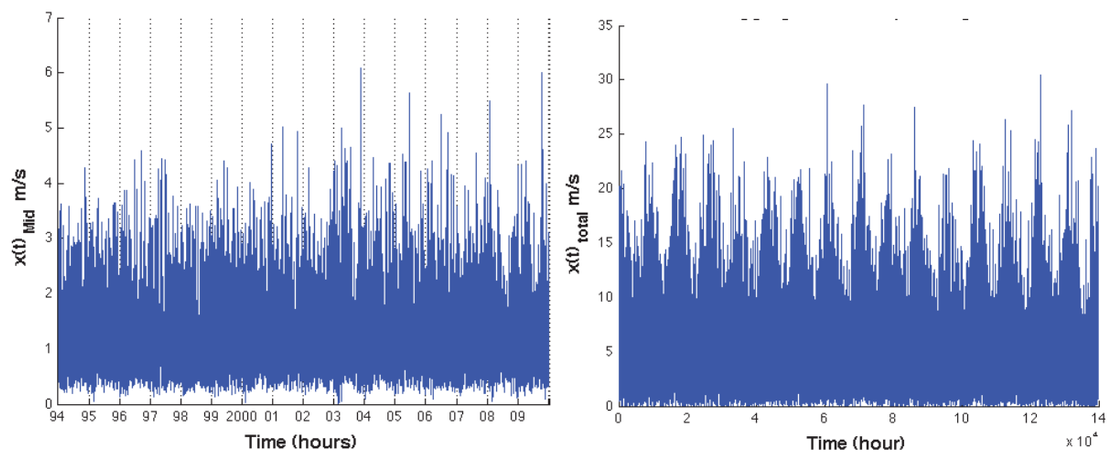

III. $x_L(t)$

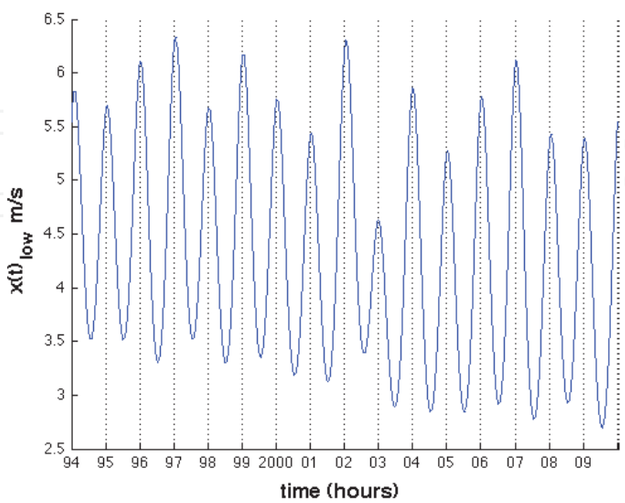

Fig. 10. Construction of wind speed signal using low, medium and high frequency components

4. Discrete Markov process

The interesting results obtained in section 2 (Figure 9) show Independencies from past observed data except for the nearest one. Model representation using Markov process is then valid, which is defined as the likelihood of next wind speed value in state *k* is conditioned on the most recent value of wind speed in state *m.* Equation (15) defines this likelihood – state relationship.

$$P(X_k = i \,|\, X_m = x_m, x_{m-1}, \ldots, X_1 = j) = P(X_k = i \,|\, X_m = x_m) \tag{15}$$

However, to identify state levels and state values, uniform midrise quantization process is carried out to discretize wind speed signal to state levels with optimum threshold or cutoffs values.

4.1 Design of optimum uniform quantizer

A midrise uniform Quantizer has been implemented that minimizes the mean square quantization error given a set of M states; we define $x = [x_1\, x_2 \cdots x_M]$ as a state value vector, and $x_t = [x_t(1) x_t(2) \cdots x_t(M-1)]$ as a quantized threshold levels or partitions vector. x is the original analog wind speed signal and x_q is the quantization signal. The quantization step Δ is defined as;

$$\Delta = x(m+1) - x(m) = x_t(m+1) - x_t(m) \tag{16}$$

The uniform Quantizer works as follows:

$$x_q = \begin{cases} x(1) & if \quad x \le x_t(1) \\ x(M) & if \quad x \succ x_t(M-1) \\ x(m)\ if\ x_t(m-1) \prec x \le x_t(m) \end{cases} \tag{17}$$

4.2 State and transition probabilities in discrete state space Markov model

Given the initial and final boundaries of each state; state probabilities can now be defined as:

$$\begin{aligned} P(m) &= P\left[x_i(m) \prec x \le x_f(m)\right] \\ &= P\left[x(m)\right] = \int_{x_i(m)}^{x_f(m)} f_X(x)\, dx \\ &= F_X(x_f(m) - F_X(x_i(m)) \end{aligned} \tag{18}$$

Where m is defined as any given state index and has the range from m= 1 to m=M. Equation (19) presents Markov linear state space model that takes prediction coefficients error signal modeled as disturbance *d,* and a regeneration time τ in which the signal updates itself, for example updates every 10 minutes (1 sample), or every one hour (6 samples) and so on.

$$x_\tau(n) = \sum_{j=1}^{N} a_j x(n-j) + d_j(n) \tag{19}$$

we define a processing time from $\tau_o \to \tau$ by a rectangular function. Equations (20) and (21) define subsequent use of state space representation.

$$x_{j,\tau}(n) = \sum_{j=1}^{N+1} a_{j+1} x(n-j) + d_j(n) \tag{20}$$

$$\overline{x_{j,\tau}}(n) = [A] \times \overline{x_{j-1,\tau}}(n) + d_j(n) \tag{21}$$

Where $[A]$ is the prediction coefficient matrix. Transition probabilities are calculated based on the counting method discussed in [11], in which we define :

$N_{trans}(k \mid m) \equiv$ The number of transitions from state m to state k in the time series,(m is the originating state, k is the next state)

$N_{state}(m) \equiv$ The number of occurrences of state m in the time series signal.

Both state and transition counters are related by (22) and the total size of the time series is defined in (23)

$$N_{state}(m) = \sum_{k=1}^{M} N_{trans}(k \mid m) \tag{22}$$

$$N = \sum_{m=1}^{M} N_{state}(m) = \sum_{m=1}^{M} \sum_{k=1}^{M} N_{trans}(k \mid m) \tag{23}$$

Using the statistical counter values of $N_{state}(m)$ and $N_{trans}(k \mid m)$, the transition and state probabilities can be statistically computed as:

$$P_{trans}(k \mid m) = \frac{N_{trans}(k \mid m)}{N_{state}(m)} \tag{24}$$

$$P_{state}(m) = \frac{N_{state}(m)}{N} \tag{25}$$

Where, *K = 1,…, M and, m= 1,…, M.* Note that (25) represent the statistical (actual) state probabilities of wind speed signal while (18) represent the theoretical state probabilities defined be either Weibull or Normal probability density functions. The probability state space representation is defined as:

$$P(\overline{x_{j,\tau}}(n)) = [P_{trans}] \times \overline{x_{j-1,\tau}}(n) \tag{26}$$

Where $[P]$ is the transition probability matrix.

In Figures 11, transition probability plots of normalized wind speed data are shown. The plots are generated from the same one-year sample size used in short term prediction (section 2). Those transition probabilities obviously appeared in cluster around the diagonal. This means smooth transitions between states and suggesting that the data does not exhibit frequent wind gusts. Moreover, we see the difference between theoretical and actual (statistical state probabilities (Figures 17 & 18). The reason is due to the use of the uniform quantization while we conjecture that a non-uniform quantizer will achieve a better match between the actual and theoretical probabilities.

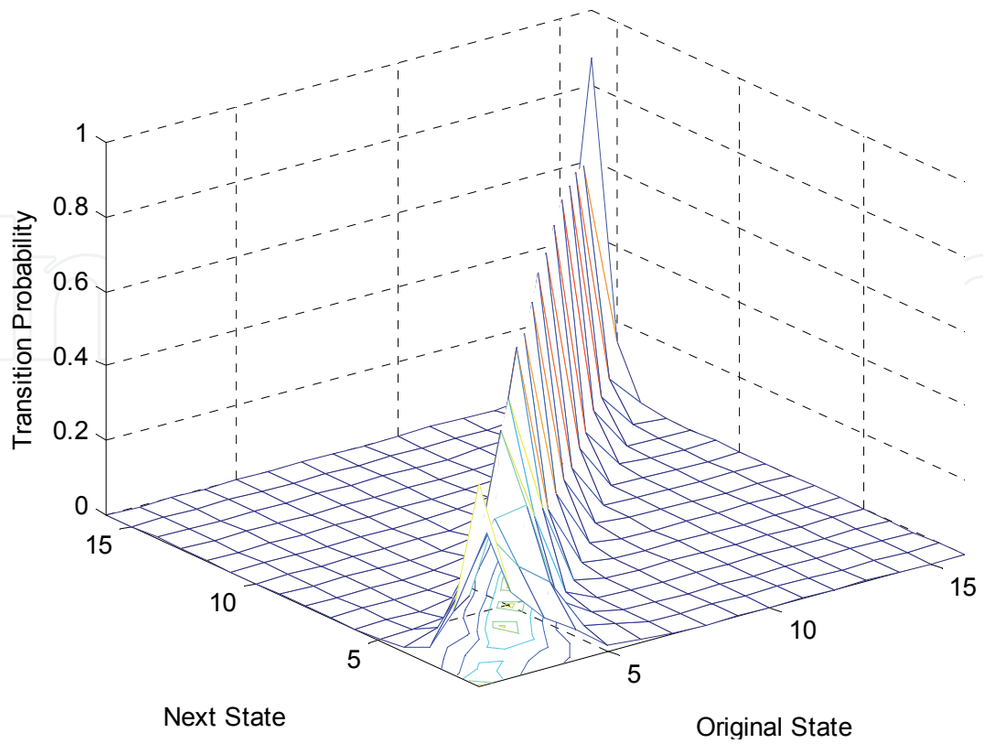

Fig. 11. Gaussian transition probabilities for M = 16 states

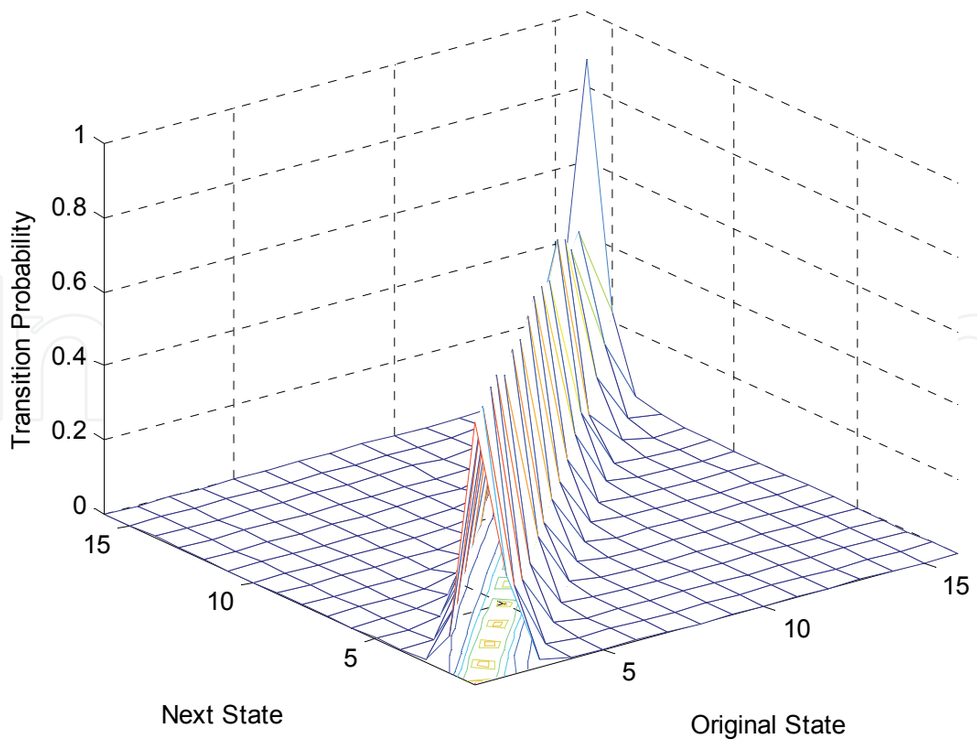

Fig. 12. Weibull transition probabilities for M = 16 states

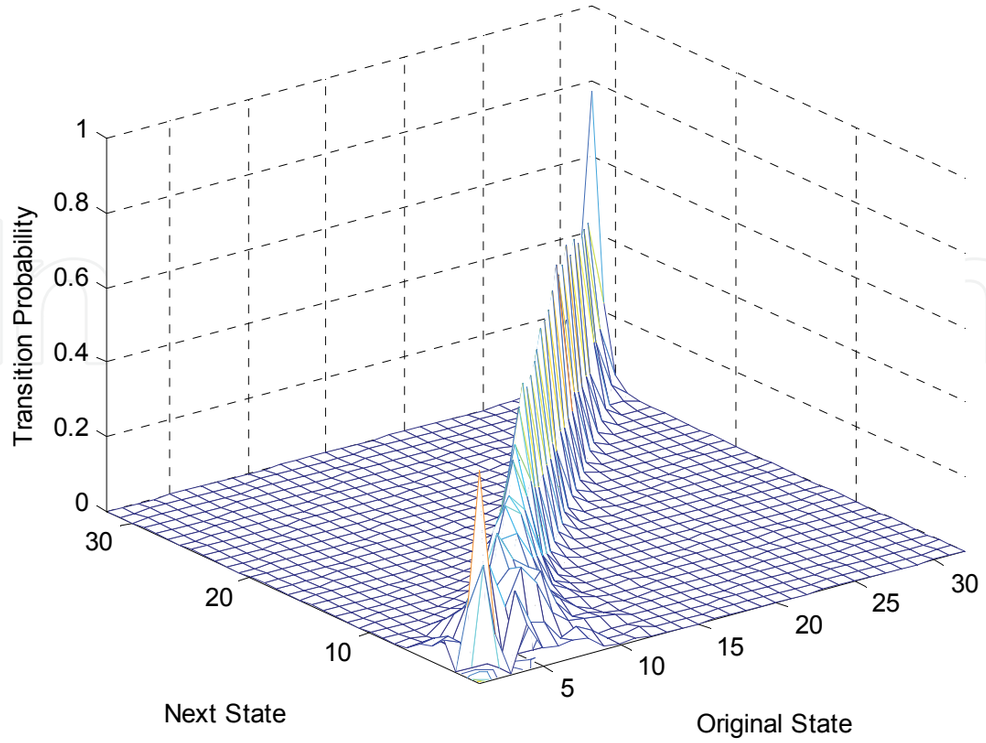

Fig. 13. Gaussian transition probabilities for M = 32 states

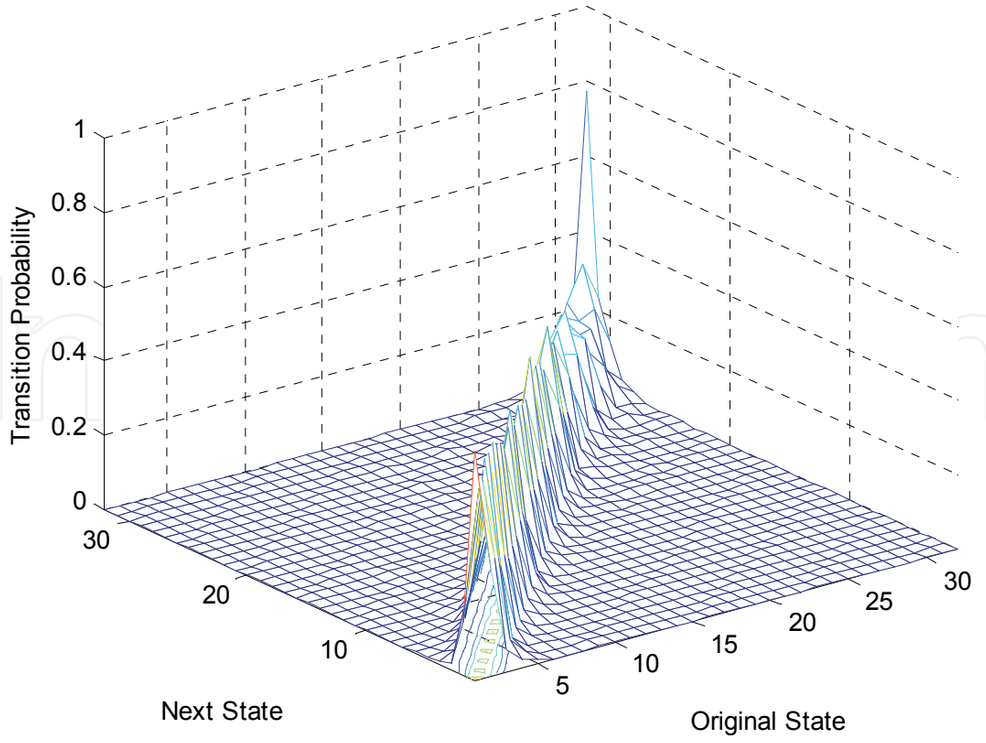

Fig. 14. Weibull transition probabilities for M = 32 states

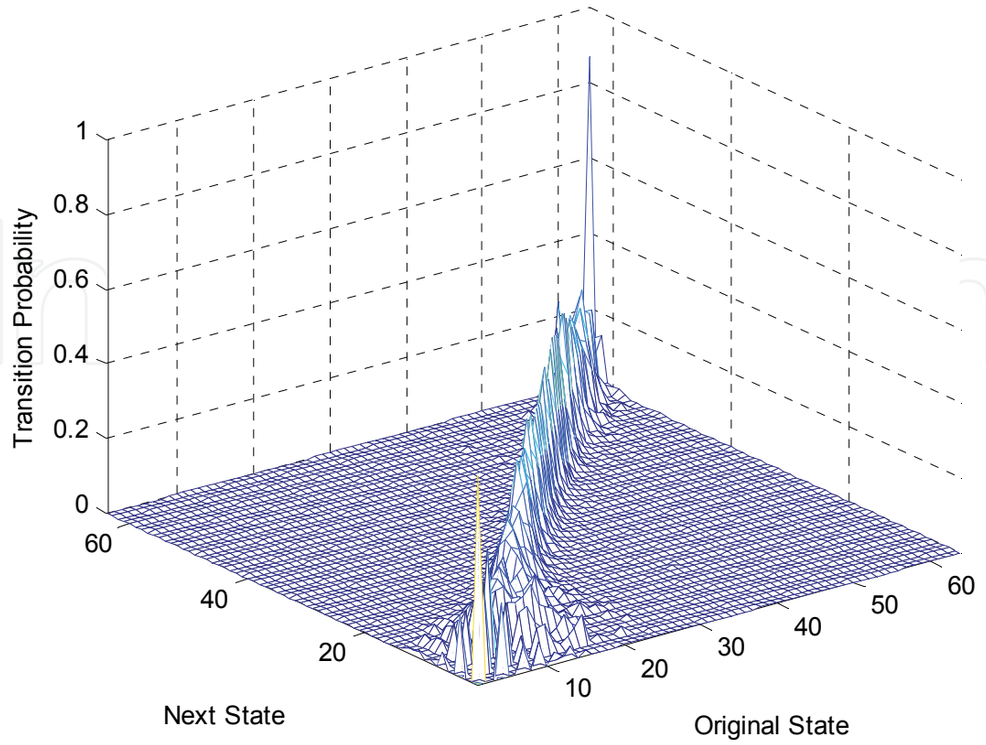

Fig. 15. Gaussian transition probabilities for M = 64 states

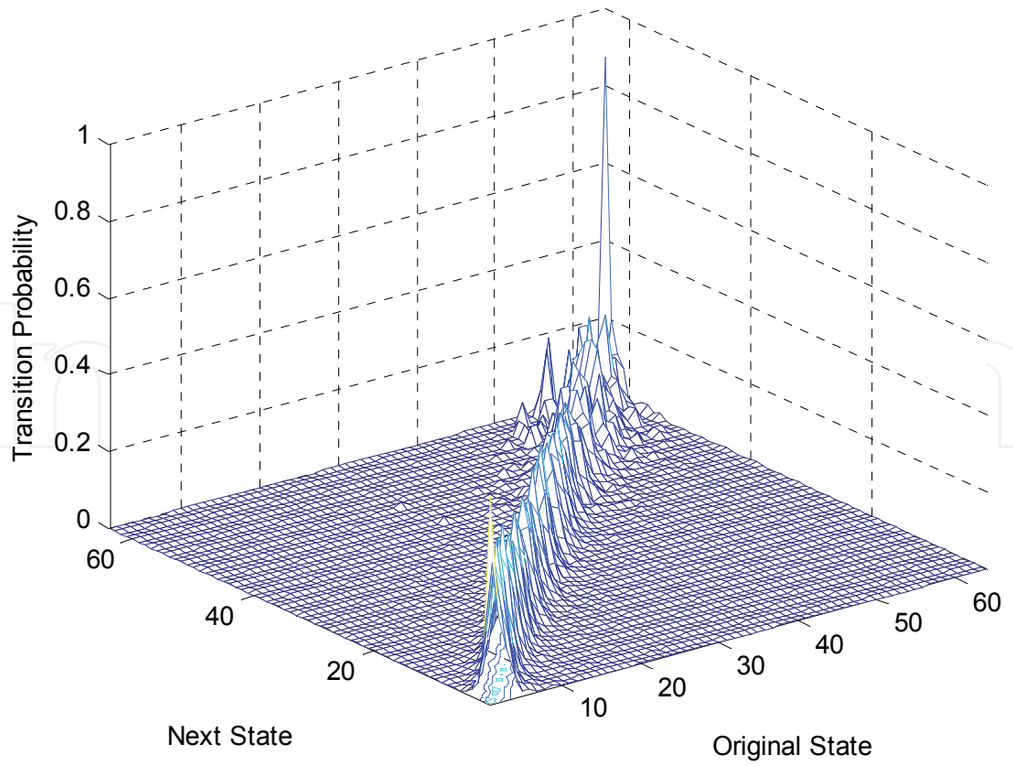

Fig. 16. Weibull transition probabilities for M = 64 states

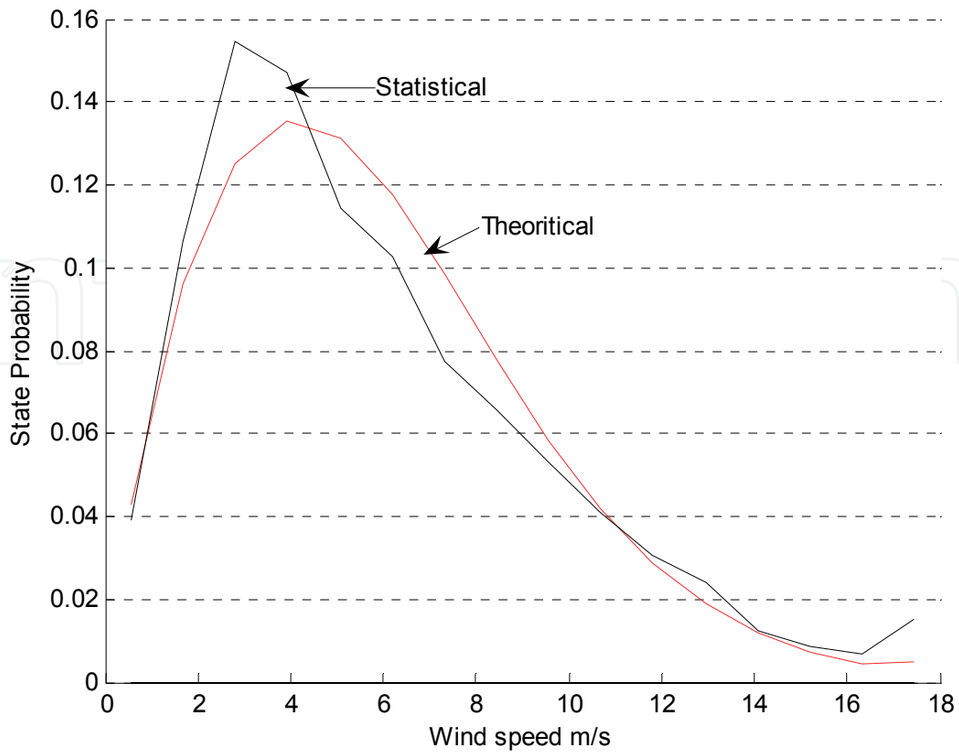

Fig. 17. Weibull state probabilities for M = 16 states

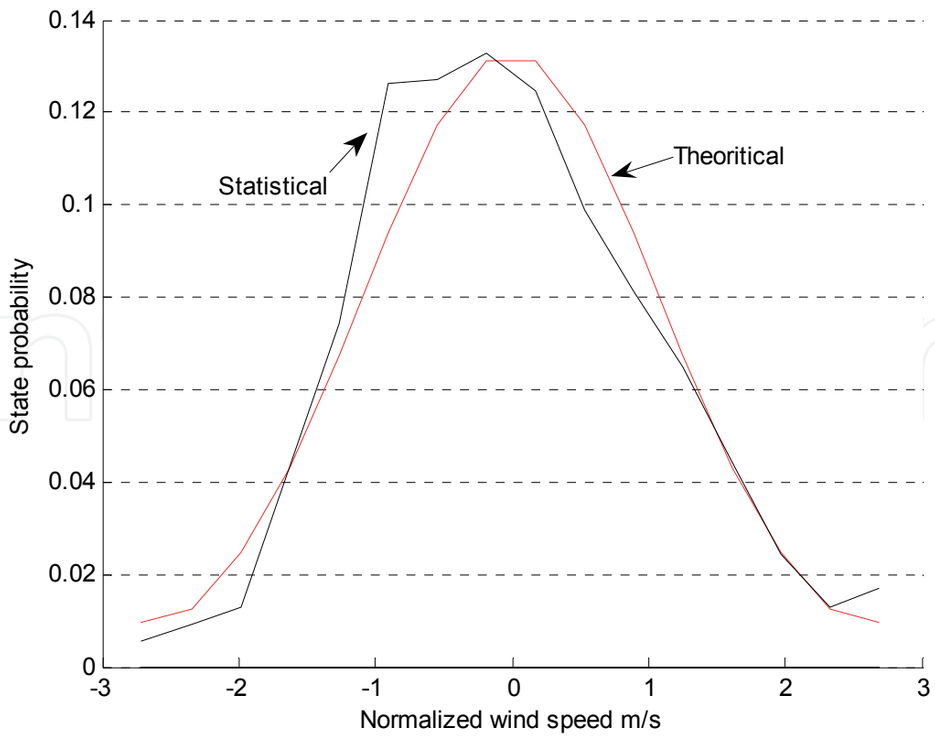

Fig. 18. Gaussian state probabilities for M = 16 states

Applying the quantization process and Markov state model to the decomposed wind speed signals presented in Figure 10 (16-year time series in hourly resolution) results in log normal distribution of wind speed state probabilities. The final results of the state probabilities are shown in Figures 19 - 21. Figures 22 – 24 show the transition probabilities for each decomposed wind speed signal. It is shown that smooth transitions appear in medium and low frequency component signals (i.e., centered around the diagonals), while high frequency component transition probabilities exhibit significant non-uniformities and disruptions due to fast changes and high frequencies variations driving the high frequency decomposed wind speed signal.

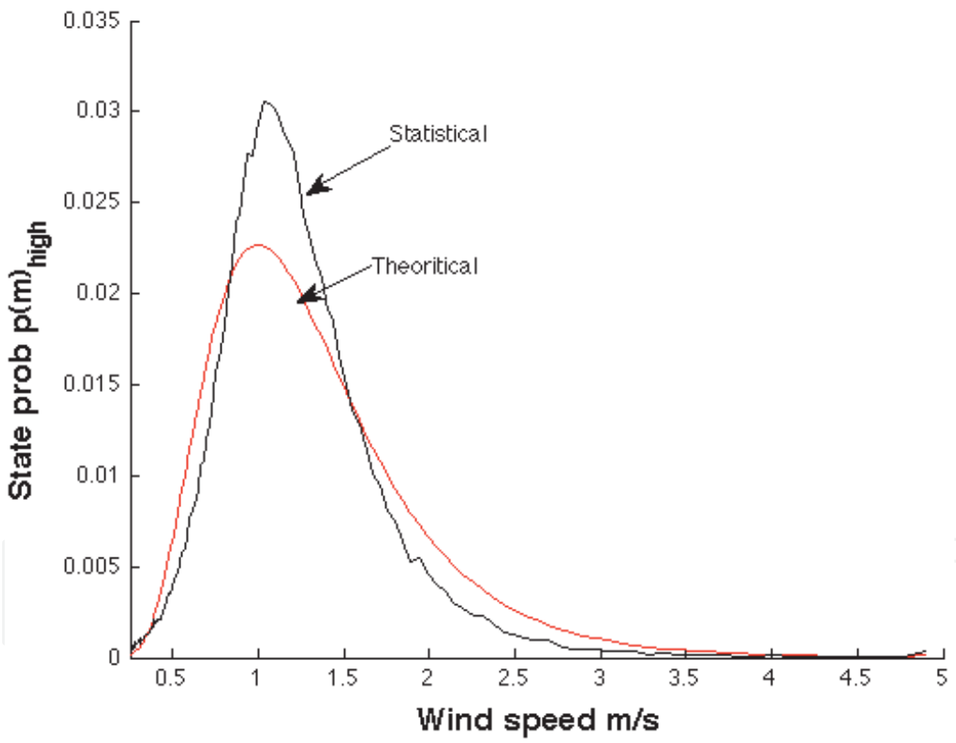

Fig. 19. Lognormal state probabilities (M = 128) for high frequency wind signal.

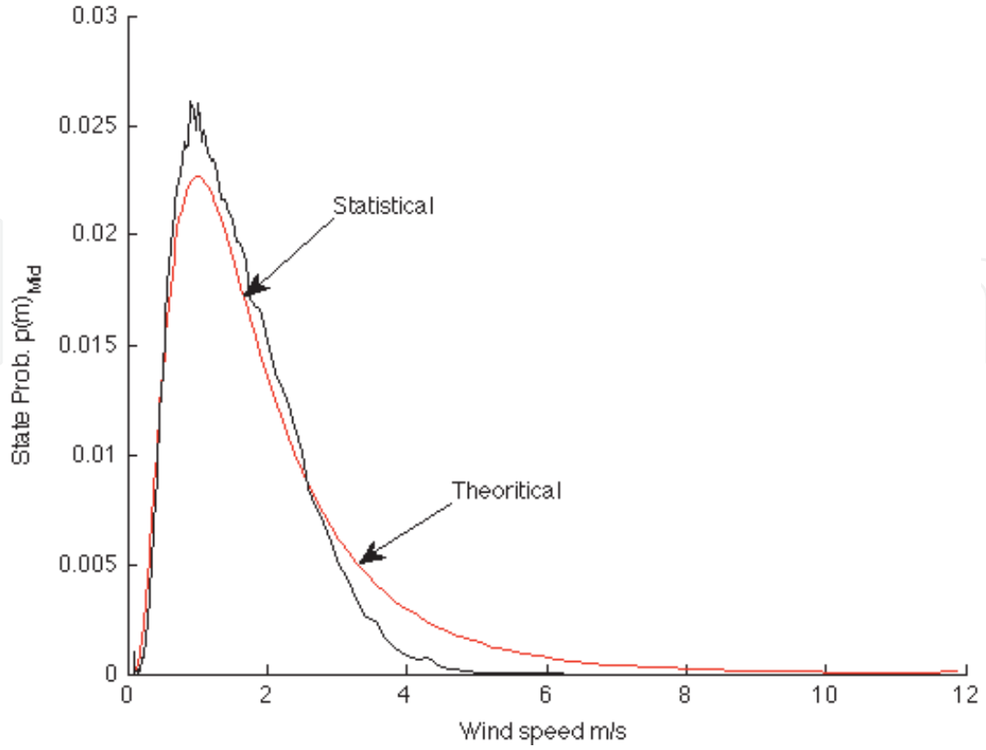

Fig. 20. Lognormal state probabilities (M = 128) for medium frequency wind signal.

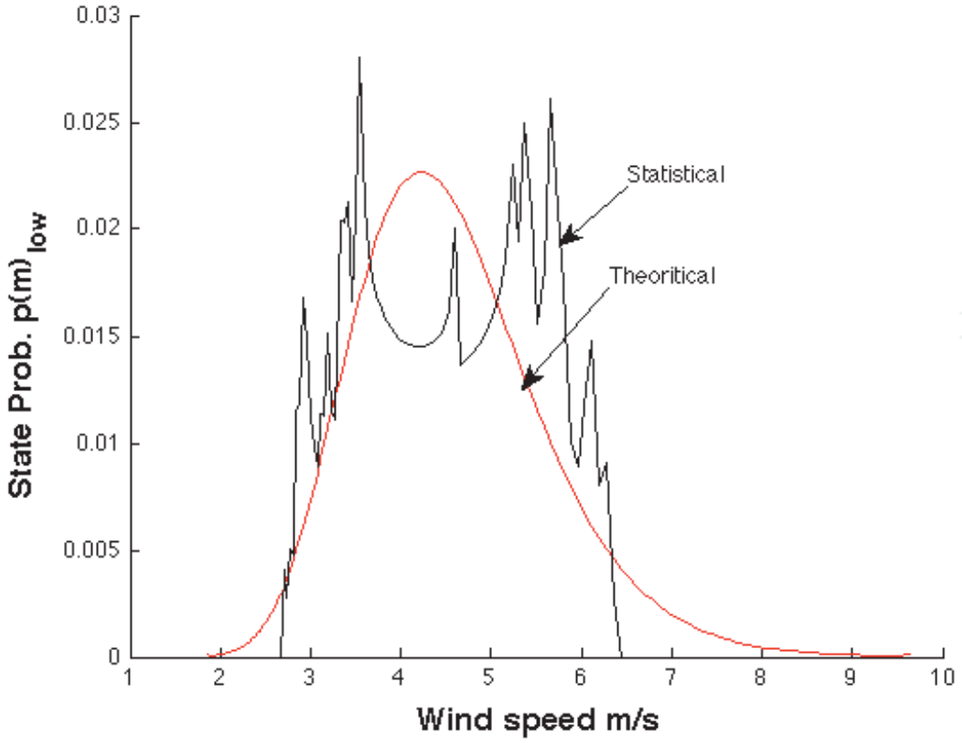

Fig. 21. Lognormal state probabilities (M = 128) for low frequency wind signal.

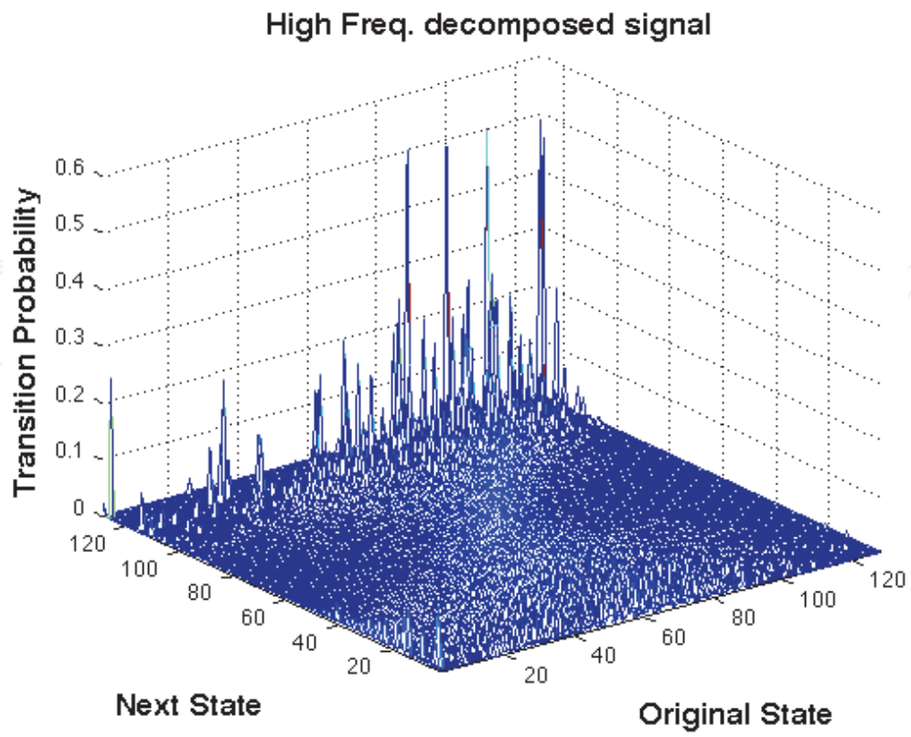

Fig. 22. Lognormal transition probabilities (M = 128) for high frequency wind signal.

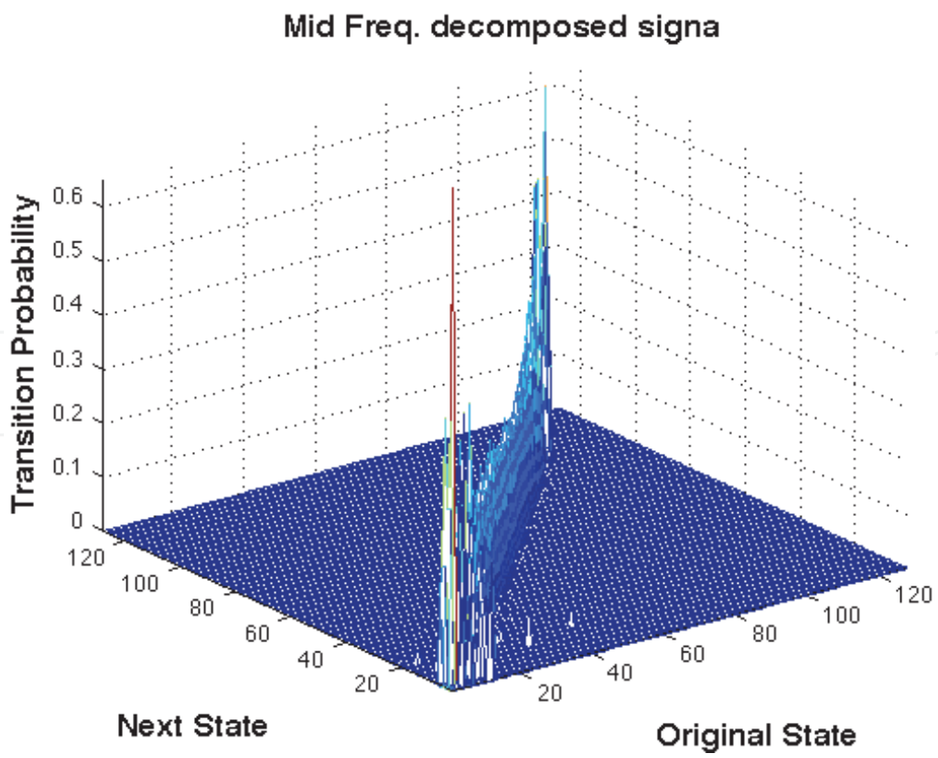

Fig. 23. Lognormal transition probabilities (M = 128) for medium frequency wind signal.

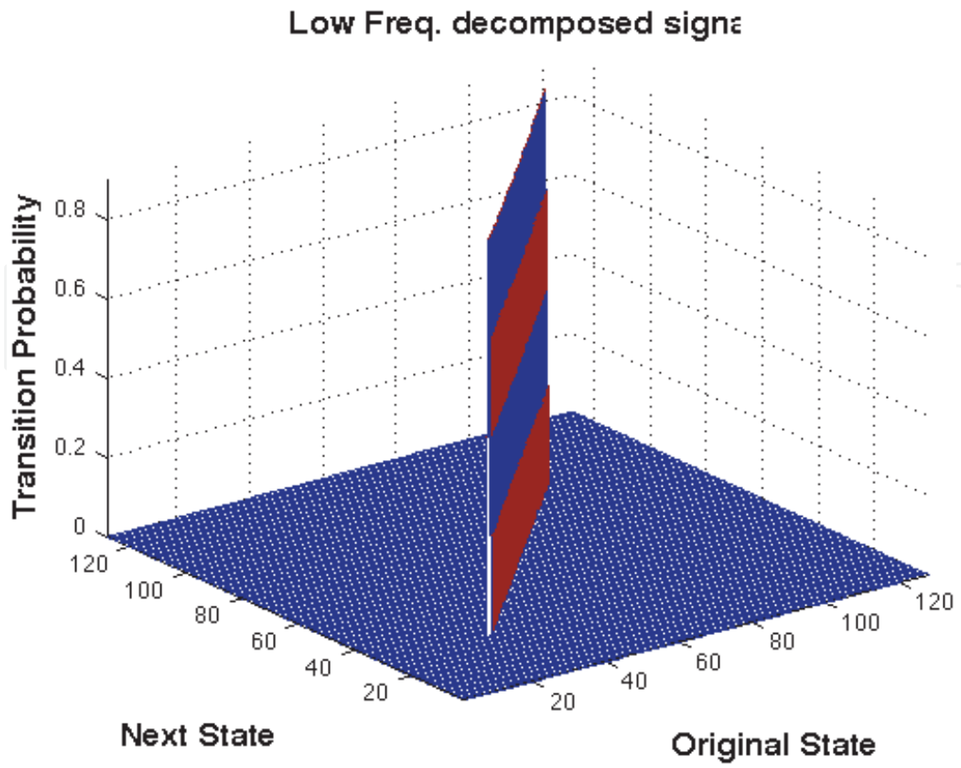

Fig. 24. Lognormal transition probabilities (M = 128) for low frequency wind signal.

5. Conclusion

This chapter characterizes wind speed signal using stochastic time series distribution models. It presents a short term wind speed prediction model using a linear prediction method by means of FIR and IIR filters. The prediction model was based on statistical signal representation by a Weibull distribution. Prediction accuracies are presented and they show independencies on past value expect for the most recent one. These in turn validate a Markov process presentation for stationary wind speed signals. The chapter also studies the integration of a complete wind speed pattern from a decomposition model using Fourier Transform for different wind time series models defined by different frequencies of each wind pattern.
Uniform quantization and discrete Markov process have been applied to the short, medium and long term wind speed time series signals. The actual state and transition probabilities have been computed statistically based on the counting method of the quantized time series signal itself. Theoretical state probabilities have been also computed mathematically using the fitted PDF model. A comparison of the statistical and theoretical state probabilities shows a good match. Both low and medium frequency signals exhibit smooth variation in state transition probabilities, while the high frequency component exhibit irregularity due to fast, short term variations.

6. References

[1] GE Energy, (March 2005), Report on "*The Effects of Integrating Wind Power on Transmission System Planning, Reliability, and Operations*" Prepared for:The New York State

Energy Research and Development Authority. Available online: http://www.nyserda.org/publications/wind_integration_report.pdf

[2] C. Lindsay Anderson, Judith B. Cardell, (2008), "Reducing the Variability of Wind Power Generation for Participation in Day Ahead Electricity Markets," *Proceedings of the 41st Hawaii Inter national Conference on System Sciences, IEEE*.

[3] Kittipong M., Shitra Y., Wei Lee, and James R., (Nov. 2007), "An Integration of ANN Wind Power Estimation Into Unit Commitment Considering the Forecasting Uncertainty," *IEEE Transactions On Industry Applications*, Vol., 43, No. 6,

[4] Marcos S. Miranda, Rod W. Dunn, (2006), "One-hour-ahead Wind Speed Prediction Using a Bayesian Methodology," *IEEE*.

[5] D. Hawkins, M. Rothleder, (2006), "Evolving Role of Wind Forecasting in Market Operation at the CAISO," *IEEE PSCE*, pp. 234 -238,

[6] Alberto F., Tomas G., Juan A., Victor Q., (Aug. 2005), "Assessment of the Cost Associated With Wind Generation Prediction Errors in a Liberalized Electricity Market," *IEEE Transactions on Power Systems*, Vol. 20, No. 3, pp. 1440-1446,.

[7] Dale L. Osborn, (2006), "Impact of Wind on LMP Market," *IEEE PSCE*, pp. 216-218.

[8] Cameron W. Potter, Micheal Negnevistsky,(2005) "Very Short-Term Wind Forecasting for Tasmanian Power Generation", IEEE, TPWRS Conference.

[9] National weather station, available online, http://www.ndbc.noaa.gov/data/5day2/DBLN6_5day.cwind

[10] B. A. Shenoi, (2006), "Introduction to Digital Signal Processing and Filter Design" John Wiley & Sons, Inc.

[11] F. Castellanos, (Aug. 2008), " Wind Resource Analysis and Characterization with Markov's Transition Maatrices," IEEE Transmission and Distribution Conf., Latin America,

[12] Noha Abdel-Karim, Mitch J. Small, Marija Ilic, (2009), "Short Term Wind Speed Prediction by Finite and Infinite Impulse

[13] Response Filters: A State Space Model Representation Using Discrete Markov Process", Powertech Conf. Bucharest, 2009.

[14] P. P. Vaidyanathan, (2008), *The Theory of Linear Prediction*, California Institute of Technology, 1st ed., Morgan & Claypool, 2008

[15] Yang HE, (2010), Modeling Electricity Prices for Generation Investment and Scheduling Analysis., Thesis proposal, University of Hong Kong.

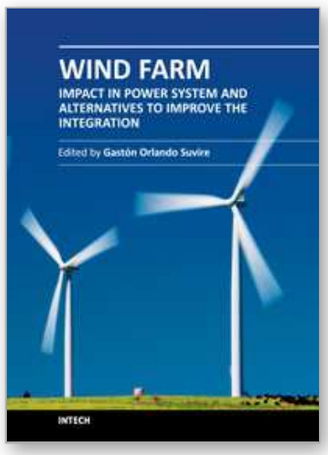

Wind Farm - Impact in Power System and Alternatives to Improve the Integration

Edited by Dr. GastÃ³n Orlando Suvire

ISBN 978-953-307-467-2
Hard cover, 330 pages
Publisher InTech
Published online 28, July, 2011
Published in print edition July, 2011

During the last two decades, increase in electricity demand and environmental concern resulted in fast growth of power production from renewable sources. Wind power is one of the most efficient alternatives. Due to rapid development of wind turbine technology and increasing size of wind farms, wind power plays a significant part in the power production in some countries. However, fundamental differences exist between conventional thermal, hydro, and nuclear generation and wind power, such as different generation systems and the difficulty in controlling the primary movement of a wind turbine, due to the wind and its random fluctuations. These differences are reflected in the specific interaction of wind turbines with the power system. This book addresses a wide variety of issues regarding the integration of wind farms in power systems. The book contains 14 chapters divided into three parts. The first part outlines aspects related to the impact of the wind power generation on the electric system. In the second part, alternatives to mitigate problems of the wind farm integration are presented. Finally, the third part covers issues of modeling and simulation of wind power system.

How to reference

In order to correctly reference this scholarly work, feel free to copy and paste the following:

Noha Abdel-Karim, Marija Ilic and Mitch Small (2011). Modeling Wind Speed for Power System Applications, Wind Farm - Impact in Power System and Alternatives to Improve the Integration, Dr. GastÃ³n Orlando Suvire (Ed.), ISBN: 978-953-307-467-2, InTech, Available from: http://www.intechopen.com/books/wind-farm-impact-in-power-system-and-alternatives-to-improve-the-integration/modeling-wind-speed-for-power-system-applications

INTECH
open science | open minds

InTech Europe
University Campus STeP Ri
Slavka Krautzeka 83/A
51000 Rijeka, Croatia
Phone: +385 (51) 770 447
Fax: +385 (51) 686 166
www.intechopen.com

InTech China
Unit 405, Office Block, Hotel Equatorial Shanghai
No.65, Yan An Road (West), Shanghai, 200040, China
中国上海市延安西路65号上海国际贵都大饭店办公楼405单元
Phone: +86-21-62489820
Fax: +86-21-62489821

IntechOpen